

A synchrotron radiation study of high-lying excited states of matrix-isolated atomic magnesium

P. Kerins, B. Healy, and J. G. McCaffrey*

Department of Chemistry, National University of Ireland, Maynooth, Co. Kildare, Ireland

(Submitted February 12, 2000; revised June 21, 2000)

Fiz. Nizk. Temp. **26**, 1016–1022 (September–October 2000)

Previous steady-state and time-resolved luminescence spectroscopy of $3p^1P_1$ atomic magnesium, isolated in thin film samples of the solid rare gases, is extended to include the higher energy $4p^1P_1$ excitation. Well-resolved site splittings are recorded in Mg/Ar samples for excitation to the $4p^1P_1$ level. A small red shift in the absorption energy to the $4p^1P_1$ level for Mg/Ar contrasts with a small blue shift on absorption to the $3p^1P_1$ level. Direct emission from the $4p^1P_1$ level is not observed in any of the rare gas matrices; instead, intense emission from the low energy $3p^1P_1$ level is. Measurements of the emission decay curves in Mg/Ar have revealed slow rates in the steps feeding the $3p^1P_1$ level following $4p^1P_1$ excitation. The reason for the differential shifting of the $4p^1P_1$ and $3p^1P_1$ levels as well as the lack of direct $4p^1P_1$ emission is thought to be related to the strong binding interaction between Mg in the $4p^1P_1$ state and the rare gases. © 2000 American Institute of Physics. [S1063-777X(00)01809-0]

1. INTRODUCTION

In recent times, the luminescence spectroscopy of matrix-isolated metal atoms, i.e., neutral metal atoms isolated at high dilution in the solid rare gases (M/RG), has been used as a sensitive probe of guest–host interactions in solid-state spectroscopy. This has arisen because of *i*) the sensitivity of these ‘‘ligand-free’’ optical centers to their host environment, *ii*) the simple, face-centered cubic (fcc) packing structures of the solid rare gases, and *iii*) the increasing availability of accurate pair potentials for several metal atom/rare gas atom (M·RG) van der Waals diatomics. Recent theoretical work¹ from the Maynooth Group on the luminescence spectroscopy of atomic zinc isolated in the solid rare gases (Zn/RG) has indicated close agreement between spectral simulations based on the use of sums of Zn·RG pair potentials² and the experimentally³ observed emission.

The spectral simulations are an extension of the theoretical methods developed by Beswick and co-workers⁴ in simulations of the vibronic spectra of gas phase metal atom-rare gas cluster species. In the solid state simulations the potential energy surfaces of the Jahn–Teller active vibrational modes of atomic Zn isolated in the solid rare gases Ar, Kr, and Xe have been calculated for a Zn·RG₁₈ cluster species. This cluster comprises the first and second spheres surrounding a guest metal atom occupying a substitutional site of an fcc lattice. Reliable calculations are possible because of the existence of detailed information on the lattice parameters of the fcc unit cells of the solid rare gases as well as accurate Zn·RG and RG·RG pair potentials. As well as indicating dominant localized interactions in the Zn/RG matrix systems, details of the microscopic motion of atomic zinc occurring during optical cycles in the solid rare gases were also obtained from simulations of the observed luminescence.

With the increasing availability of accurate diatomic interaction potentials, obtained from laser spectroscopy of

metal atom-rare gas atom (M·RG) van der Waals complexes in supersonic expansions,⁵ the range of systems, including open-shell systems, amenable to this detailed analysis is steadily growing. One of the most interesting examples in this regard is the recent observation made by Breckenridge and co-workers⁶ on the doubly excited Mg($3p_\pi 3p_\pi^3 P_J$)·RG [$^3\Sigma^-$] valence states of the Mg·RG diatomics (RG=He, Ne, Ar and Kr) accessed from the singly excited Mg($3s_\sigma 3p_\pi^3 P_J$)·RG [$^3\Pi$] metastable state. Theoretical analysis of the very strong binding energy ($D_0 = 2850 \text{ cm}^{-1}$) and short bond length ($R_0 = 2.41 \text{ \AA}$) in the molecular $^3\Sigma^-$ state of Mg·Ar, arising from the doubly excited ($3p$)² atomic magnesium configuration, indicates the importance of the absence of occupied metal *s* orbitals in the interaction with the closed shell rare gas atom. Partial occupancy of the $3s$ orbital in the lower-energy $3s3p$ metal atom valence state is responsible for increased repulsive interaction with the rare gas atom, giving rise to a greatly reduced binding energy (160 cm^{-1}) and an increased bond length (3.66 \AA) for the Mg($3s_\sigma 3p_\pi^3 P_J$)·Ar [$^3\Pi$] metastable state. Full occupancy of the $3s$ orbital in the Mg($3s_\sigma 3s_\sigma^1 S_0$)·Ar [$^1\Sigma$] ground electronic state results in the molecular parameters.⁷ $D_0 = 65 \text{ cm}^{-1}$ and $R_0 = 4.5 \text{ \AA}$, typical of van der Waals complexes. Comparison of the larger binding energy and shorter bond length of the neutral Mg·Ar ($3p_\pi 3p_\pi^3 P_J$) [$^3\Sigma^-$] state with the analogous values ($D_0 = 1240 \text{ cm}^{-1}$ and $R_0 = 2.82 \text{ \AA}$) in the ground Mg⁺($3s_\sigma^2 S$)·Ar [$^2\Sigma^+$] state of the Mg⁺·Ar cation, reveals the repulsive role played by the occupied $3s$ orbital in the bonding. Significantly, these results indicate the dominance of the repulsive *s* orbital interaction over the strongly attractive, dipole-induced interaction expected in the molecular cation.

It should be revealing, on several levels, to record the luminescence spectroscopy of highly excited states for matrix-isolated Group 2 and 12 metal atoms and compare data with the pair-potentials methods used for the spectral

simulation of lower-energy metal atom transitions. The areas of interest in such a comparison are:

—Considering the strong binding energies in highly excited states, is the occurrence of many-body effects manifested?

—Due to these states being within a few thousand wave numbers of the ionization limit of the metal atom, does the onset of delocalized behavior, such as exciton absorption, occur?

—Is the localized approach taken in the present cluster-based simulations valid for these strongly bound states?

—Is metal atom migration possible in these excited states, considering that the energy minima of the highly excited states are at very short bond lengths?

The metastable atoms, generated in copious amounts with the laser ablation technique used in the gas phase for producing metal vapor, are absent in low-temperature matrices, irrespective of the method used to generate the metal vapor. Therefore the one-photon techniques used in the gas phase are not of use in matrix work on doubly excited states. Instead of looking at the doubly excited states, we have examined the one-photon spectroscopy of high-lying, singly excited atomic states. In the present contribution the matrix luminescence of the $3p^1P_1$ state of atomic magnesium is extended in that excitation spectra have been recorded in the vacuum UV spectral region to reach the $4p^1P_1$ energy level.

Notwithstanding the vacuum spectroscopic techniques required to reach highly excited levels, the reduced oscillator strength of atomic transitions from the ground state to these states is a more fundamental deterrent to such measurements. In the case of Mg, for example, the transition probability of the $4p-3s$ singlet transition at 202.58 nm is $A = 0.84 \times 10^8 \text{ s}^{-1}$, almost an order of magnitude smaller than the A value⁸ of $4.95 \times 10^8 \text{ s}^{-1}$ for the $3p-3s$ singlet transition at 285.21 nm.⁹ The use of synchrotron radiation (SR), with output intensities optimized in the VUV spectral region, compensates the reduced transition probabilities and, as it is already produced under ultrahigh vacuum conditions, facilitates the measurement of high-lying excited states.

Studies of the absorption spectroscopy of matrix-isolated metal atoms are quite comprehensive and well documented. Conversely, luminescence studies of the excited states of metal atoms are not nearly as extensive, but detailed studies¹⁰ have been carried out for the lighter elements of the Group 1, 2, 11, and 12 elements. The first study of matrix-isolated atomic magnesium was that of Schnepf,¹¹ in which optical absorption spectra were recorded at 4.2 K using argon, krypton, and xenon as host materials. Schatz *et al.*¹² measured the MCD spectra of magnesium isolated in argon, and more recently the luminescence of matrix-isolated magnesium was recorded by McCaffrey and Ozin¹³ in argon and krypton at 12 K. The latter work agreed with the absorption data of Schnepf in that the excitation bands observed in the vicinity of 285 nm and assigned to the $3p^1P_1 \rightarrow 3s^1S_0$ singlet transition of atomic magnesium all exhibited three-fold splitting.

With the objective of extending the experimental data base on the luminescence spectroscopy of matrix-isolated metal atoms the spectroscopy of metal atoms in highly excited states has been undertaken using SR as the excitation

source. The paper is structured as follows. Transitions to and from the $3p^1P_1$ energy level for the cases of Mg/Ar, Mg/Kr, Mg/Xe, and Mg/CF₄ will be reviewed briefly before the new data on the $4p^1P_1$ energy levels is presented. Because of the large signal strengths of the transitions observed in Mg/Ar, much of the detailed presentation will involve this system. Key differences in the spectroscopy of the $3p^1P_1$ and $4p^1P_1$ states will be highlighted and discussed.

2. EXPERIMENTAL

Thin film Mg/RG samples were prepared by the cocondensation of magnesium vapor, with the rare gases onto an LiF window. The metal vapor was produced by electron bombardment of 0.5 mm thick Mg foil (Goodfellow, 99.99% purity) coiled into a 5 mm diameter molybdenum crucible in an Omicron EFM3 UHV evaporator. Preferential isolation of atoms over metal clusters was achieved using very low metal fluxes (<1 nA), and the isolation condition of samples was monitored by recording absorption spectra. Cryogenic temperatures were achieved with a Cryovac continuous-flow liquid-helium cryostat. The sample temperature was measured with a silicon diode mounted on the sample holder and set using a Lakeshore Cryotronics model 330 temperature controller. Deposition temperatures of 5, 12, 18, and 25 K were used with the rare gases Ne, Ar, Kr, and Xe, respectively.

An MKS 221A Baratron capacitance manometer, sensitive in the pressure range 0–1000 mbar, was employed to monitor the amounts of rare gas admitted to the gas handling system and consumed during sample formation. The UHV sample chamber containing the liquid-helium cryostat was pumped continuously with a Pfeiffer/Balzers TPU 240 turbomolecular pump. Vacuum, monitored with an HPS Division/MKS Series 423 I-Mag cold cathode gauge, was typically in the mid 10^{-10} mbar range prior to cool-down, dropping to 10^{-11} mbar after cool-down. Gas flow rates, controlled by a Granville-Phillips series 203 variable leak valve, were generally in the range of 3.5 to 5 mmol/h for periods of between 20 to 30 minutes. This resulted in the formation of thin film samples whose thickness was in the 30–50 μm range. Rare gases of 99.999% purity were used as supplied by Linde Technische Gase.

Since the optical layout of the HIGITI apparatus located at HASYLAB/DESY in Hamburg has been presented in our earlier work,³ only a brief description will be given here. Synchrotron radiation optimized in the VUV spectral region was used as the excitation source. Absorption spectra were recorded by monitoring the amount of UV radiation directly transmitted through the Mg/RG samples, using a Valvo XP2020Q photomultiplier tube to detect the visible emission of a sodium salicylate UV-to-visible converter. All spectra were recorded linear in wavelength, but for purposes of analysis and discussion are presented linear in photon energy, in wave number units (cm^{-1}).

Luminescence measurements were made in the VUV spectral region with a modified 1 m Wadsworth monochromator for excitation, and a 0.4 m Seya-Namioka monochromator for emission. A Hamamatsu MCP 1645U-09 microchannel plate was used for photon detection. Nanosecond lifetime measurements were made using the time correlated

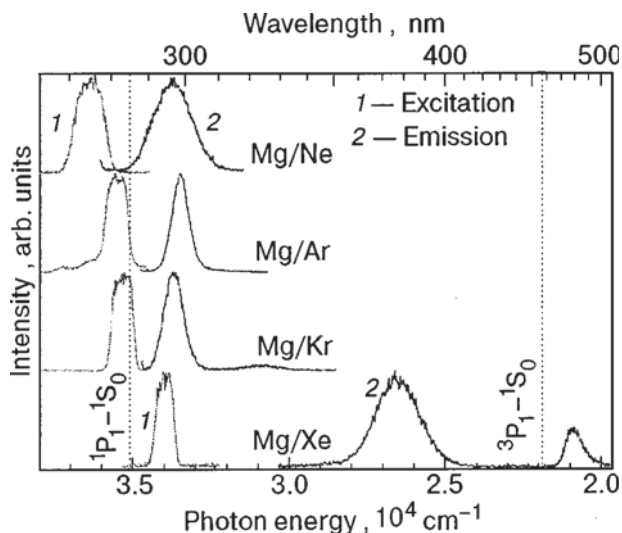


FIG. 1. A summary of the matrix luminescence spectroscopy recorded at 6 K for the $3p-3s$ transitions of atomic magnesium isolated in annealed samples of the solid rare gases Ne, Ar, Kr, and Xe. Excitation spectra are denoted as 1, while emission spectra are denoted as 2. The locations of the spin singlet $3p^1P_1 \leftarrow 3s^1S_0$ and triplet $3p^3P_1 \leftarrow 3s^1S_0$ transitions of atomic magnesium in the gas phase are given by the vertical dotted lines. Noteworthy in Mg/Ar is the presence of multiple features between 270 and 280 nm in the excitation spectra of annealed samples.

single photon counting (TCSPC) technique.¹⁴ The synchrotron radiation¹⁵ generated from the DORIS III storage ring at HASYLAB/DESY has a temporal profile of 120 ps (FWHM), and when provided in “5 Bunch Mode,” at a repetition rate of 5.208 MHz, decay times of up to 10 μ s can be measured with TCSPC. Decay times were extracted by fitting trial functions, single, double or triple exponential functions, convoluted with the temporal profile of the SR excitation pulse, to the recorded decay profiles. The reconvolution and fitting was achieved using the “ZFIT” program¹⁶ running on DEC Alpha 3000/500 AXP workstations in Maynooth and Hamburg. The fitting criterion was based on an optimization routine minimizing the sum of weighted residuals existing between the fit and the data set. The quality of a fit can be judged numerically by the χ^2 value obtained—in our fits the acceptable range was 0.98 to 1.1.

3. RESULTS

Luminescence from the $3p^1P_1$ level

Figure 1 presents a summary of the luminescence spectroscopy recorded at 6 K for the low-energy $3p^1P_1$ state of atomic magnesium isolated in the annealed solid rare gases. The spectra (1) shown in Fig. 1 are the excitation spectra recorded by monitoring the emission bands (2). Also shown in Fig. 1 are the locations of the singlet $3p^1P_1-3s^1S_0$ and triplet $3p^3P_1-3s^1S_0$ transitions of atomic magnesium in the gas phase.⁹ Based on the spectral locations, the emission bands in the Ne, Ar, and Kr systems can be assigned to the singlet transition. Measurement of the radiative decay times of the emission bands at 370 and 470 nm in Mg/Xe has allowed assignment¹⁷ of the latter band to the triplet $3p^3P_1$ and the former, to the singlet. Lifetime

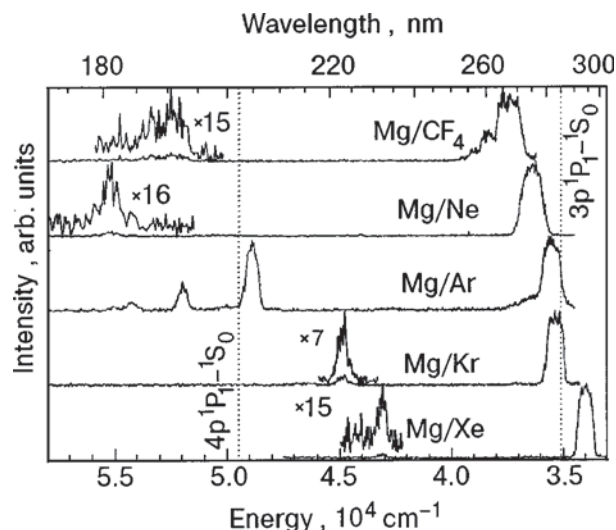


FIG. 2. A summary of the higher-energy $4p^1P_1$ bands and lower-energy $3p^1P_1$ excitation bands recorded by monitoring the $3p^1P_1 \rightarrow 3s^1S_0$ emission of atomic magnesium in the rare gases and CF_4 . The excitation spectra have not been corrected for the wavelength-dependent output intensity of the synchrotron radiation source.

measurements of the emission present in the Mg/Ne,¹⁸ Mg/Ar, and Mg/Kr systems¹³ confirm the singlet assignments suggested by their spectral locations.

Luminescence from the $4p^1P_1$ level

When the excitation spectra of the singlet $3p^1P_1-3s^1S_0$ emission bands shown on the right in Fig. 1 were recorded into the vacuum-UV region, the results shown in Fig. 2 were obtained for the annealed Mg/RG systems and Mg/ CF_4 . The location of the singlet $4p^1P_1-3s^1S_0$ transition in the gas phase is also shown. It is evident in Fig. 2 that the most intense feature in the Mg/Ar system is observed in the vicinity of the gas phase $4p^1P_1$ transition. The Mg/Ar system exhibits three well-resolved peaks, a dominant band at 204.5 nm, another at 192.5 nm, and a weak one at 185 nm. Manifestation of multiple, non-resolved features are also present at 270 nm, on the blue wing of the lower $3p^1P_1$ band. Single peaks can be seen in Ne at about 182 nm, Kr at about 221 nm, and in Xe at 231 nm. The single short-wavelength peaks in the M/RG systems parallel the single bands present on the $3p^1P_1-3s^1S_0$ transition shown on right-hand side. Because of the spectral richness in the Mg/Ar system, annealing studies were undertaken to facilitate assignment. With the large emission intensity in this system, detailed kinetic measurements have also been made.

Mg/Ar on deposition

The complete excitation spectrum of the Mg/Ar 299 nm emission is presented in the lower portion of Fig. 3 as recorded for a freshly deposited sample. Five resolved excitation bands can be seen in the high-energy region. The positions of these bands are at 226.7, 214, 204.5, 192.5, and 185 nm. An ill-defined number of unresolved features are also present on the lower energy $3p^1P_1-3s^1S_0$ excitation spectrum between 270 and 290 nm. The emission spectrum shown on the right was produced with 282 nm excitation.

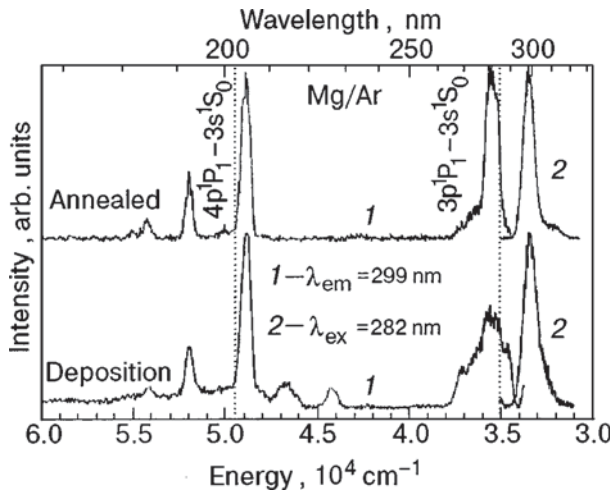


FIG. 3. Excitation bands recorded for magnesium atom emission at 299 nm in argon matrices before and after annealing. The emission bands shown on the right were produced with excitation at 282 nm. The gas phase positions of the singlet $4p^1P_1 \leftarrow 3s^1S_0$ and singlet $3p^1P_1 \leftarrow 3s^1S_0$ transitions are shown by the vertical lines.

The results of annealing studies, used to identify the origin of the resolved high-energy features, are now presented.

Mg/Ar annealed

The upper portion of Fig. 3 shows all the excitation bands of Mg/Ar recorded for the 299 nm emission after sample annealing to 32 K for 30 minutes. From a comparison of the two panels in Fig. 3, one can see that the bands at 226.7 nm and 214 nm in the spectrum of a freshly deposited sample are completely removed with annealing. Moreover, an underlying contribution to the baseline in the freshly deposited scan has been removed. This behavior is accompanied by the removal of the 290 nm red-wing features on the $3p^1P_1$ excitation band (2) in Fig. 3.

Emission bands produced from each of the excitation features (204.5, 192.5, and 185 nm) remaining after annealing all have a maximum intensity at 298 nm, but, as shown in Fig. 4, they have a varying intensity in the red wing. It should be pointed out that with high energy 204.5, 192.5,

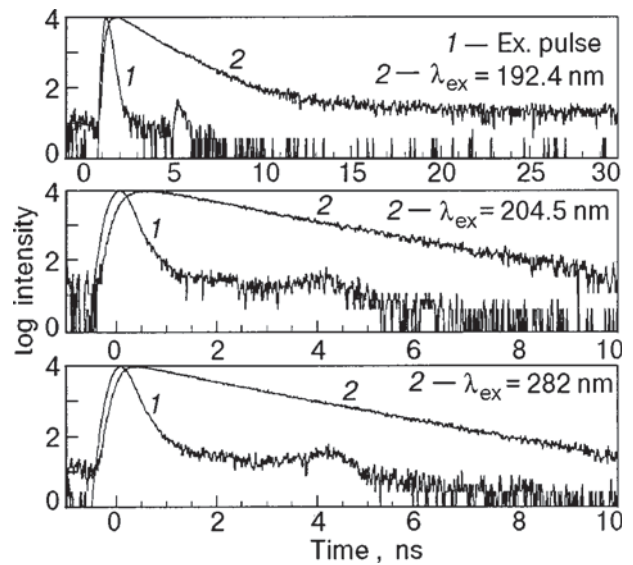
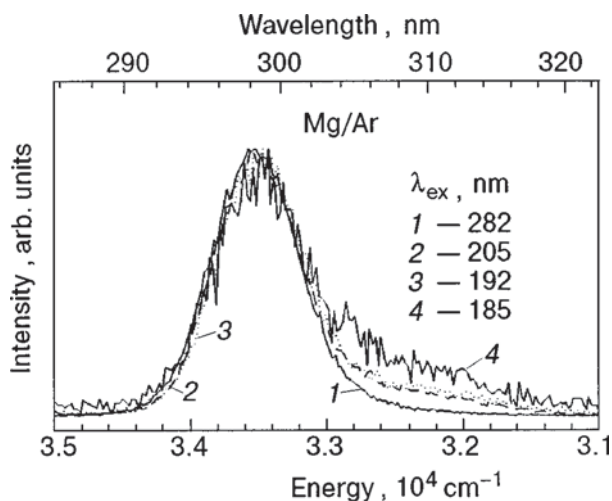


FIG. 5. Semi-log plots of the intensity decay profiles recorded for the 298 nm emission band produced with excitation of the three dominant excitation bands present in annealed Mg/Ar samples. The temporal profile of the synchrotron radiation excitation pulse is shown as (1), while (2), showing a gradual decrease in intensity, is the decay profile.

and 185 nm excitation, no emission was observed in the low 200 nm region which would correspond to direct $4p^1P_1 \rightarrow 3s^1S_0$ emission.

Figure 5 shows the decay profiles recorded for the 299 nm emission with the TCSPC technique by exciting at 282, 204.5, and 192.4 nm. The decay profiles for the 282 and 204.5 nm excitation are presented in a 10 ns time range, while the 192.4 nm excitation is shown in a 30 ns range. The simplest decay profile is exhibited by 282 nm excitation, i.e., from the direct $3p^1P_1 \leftarrow 3s^1S_0$ transition. As the excitation energy increases, the shape of the profiles changes under the influence of the associated rise times and long decay components. Table I lists the decay times and rise times extracted from fits to the emission decay curves. In agreement with earlier work,¹³ the radiative decay time of the 299 nm emission produced with $3p^1P_1$ excitation at 282 nm is found to be 1.4 ns. This is represented by τ_1 in Table I and found to be present in the emission decay curves recorded for all three excitation wavelengths. The decay curve produced with excitation at 204.5 nm exhibits a rise time of 0.27 ns, which produces the delayed appearance of the profile shown in the middle panel of Fig. 5. Excitation at 192.4 nm results in the same rise time (0.22 ns) but with a long decay component of 20.8 ns in addition to the 1.4 ns radiative decay time. A summary of the decay kinetics is presented in Fig. 6.

TABLE I. Emission decay times measured at 6 K with the TCSPC technique by exciting into the high energy bands observed for magnesium in argon. The wavelengths listed are in units of nm, the decay times are in ns. Rise times are shown underlined. The percentage yields of all the observed components are also shown.

λ_{ex}	λ_{em}	τ_1	τ_2	τ_3	%(1)	%(2)	%(3)
282	299	1.46	—	—	100	—	—
204.5	299	1.46	<u>0.27</u>	—	89.3	10.7	—
192.4	299	1.43	20.8	<u>0.22</u>	86.2	4.6	9.17

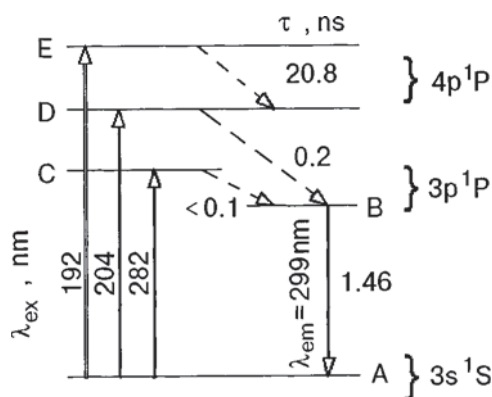


FIG. 6. A kinetic scheme of the relaxation process of the $4p^1P_1$ excited state leading to emission from the lower-energy $3p^1P_1$ level. Radiative transitions are shown by solid lines, nonradiative transitions connecting the excited state levels are represented by broken lines. The time constant of the nonradiative process connecting the absorbing (282 nm) and emitting level (299 nm) in the $3p^1P_1$ state is faster than the 0.1 ns temporal resolution of the measuring system. Level E is a resolved site splitting on the $4p^1P_1$ excited state.

4. DISCUSSION

Mg/Ar has three high-energy excitation bands in the vicinity of 200 nm, which have been shown in annealing studies (see Fig. 3) to be thermally stable. Examination of the term diagram for atomic magnesium reveals that for energies less than $50,000\text{ cm}^{-1}$ the states to be considered in the assignment of these bands are $4s^1S$ and 3S , $3d^1D$ and 3D , $4p^1P$ and 3P . Of these states the spin triplets can be ruled out in absorption (excitation) transitions from the singlet $3s^1S$ ground state. Of the spin singlets the $4s^1S$ level at 43503 cm^{-1} (229.9 nm) and the $3d^1D$ level at 46403 cm^{-1} (215.5 nm) are parity-forbidden in transitions from the ground S state, leaving the $4p^1P$ level as the only one which can couple with a large oscillator strength ($A=0.84 \times 10^8\text{ s}^{-1}$) to the ground state. The $4p^1P_1 \leftarrow 3s^1S_0$ transition of atomic magnesium, which occurs in the gas phase⁶ at 202.6 nm is, because of its spectral proximity and its fully allowed nature, the obvious assignment, especially for the 204.5 nm band in Mg/Ar.

However, it has been observed in earlier matrix work on atomic calcium that the transition to the 1D level, which is parity-forbidden in the gas phase, becomes partially allowed in the matrix. This effect has been observed in absorption¹⁹ and excitation²⁰ work and is thought to arise from metal atom occupancy in low-symmetry sites. It has also been noted that the matrix shifts on the $3d^1D_2 \leftarrow 4s^1S_0$ transition are much smaller than on the corresponding $4p^1P_1 \leftarrow 4s^1S_0$ transition and, as expected, the absorption strengths of the former transition are about two orders of magnitude less than the fully allowed $^1P_1 \leftarrow ^1S_0$ transition. Given that the gas phase $3d^1D - 3s^1S$ transition of atomic magnesium occurs at 46403 cm^{-1} (215.5 nm), a large blue shift of 2487 cm^{-1} would result for a $3d^1D_2$ assignment of the 204.5 nm (48900 cm^{-1}) band in argon matrices. It might be argued that this blue shift arises from a dominant Rydberg character in the $3d$ orbital. However, it is known that a blue shift of only 399 cm^{-1} occurs on the associated $3p^1P$ state of Mg in Ar whose n orbital would be expected²¹ to have a more character than the $3d$ orbital.

Given the strength of the three spectrally resolved high-energy excitation bands in the Mg/Ar system and their correspondence with features which are present but not resolved on the high-energy side of the $3p^1P_1$ excitation band (around 270 nm), the high-energy features are tentatively assigned as $4p^1P_1 \leftarrow 3s^1S_0$ excitations arising from multiple site occupancy of atomic magnesium in argon. Of the three excitation bands, the $4p^1P_1$ level assignment of the dominant band at 204.5 nm is the most definitive because of its close proximity to the gas phase line at 202.58 nm.⁶ This matrix transition therefore exhibits a small red shift of -463 cm^{-1} from the gas phase $4p^1P_1 \leftarrow 3s^1S_0$ transition. In contrast, the 282 nm transition to the $3p^1P_1$ level is blue-shifted by $+399\text{ cm}^{-1}$ from the corresponding gas phase value at 285.21 nm. This differential shifting of the excitation energies for the two transitions is quite revealing, since they share the same ground state. This suggests that slight repulsion dominates the Mg($3p^1P_1$)/Ar interaction, while a slight attraction dominates the Mg($4p^1P_1$)/Ar interaction.

Decay times of the emission produced with excitation of the three high energy bands are presented in Table I. From the common 1.4 ns decay time exhibited by all three emissions, and given that this is the radiative lifetime of the $3p^1P_1$ level, it can be stated that the terminating emitting level reached in relaxation from the $4p^1P_1$ level is the $3p^1P_1$ level. The mechanism of this electronic energy relaxation is not known, but assuming a strongly attractive Mg($4p^1P_1$)/Ar interaction, it probably involves a curve crossing of a deeply bound Mg($4p^1P_1$)·Ar¹Π state by a repulsive Mg($3p^1P_1$)·Ar¹Σ curve dissociating to the $3p^1P_1$ state. The efficiency of this process can be judged by the fact that the emission from the $4p^1P_1$ level is completely quenched. An assessment of the proposed relaxation mechanism awaits collection of spectroscopic data on the Mg($4p^1P_1$)·Ar¹Π state of the 1:1 van der Waals complex. However, the analogous doubly excited Mg($3p^2P_J$)·Ar³Σ state has revealed very strong binding interactions, but matrix data has not yet been obtained on transitions reaching this state.

5. CONCLUSIONS

Excitation spectra have been recorded in the vicinity of the $4p^1P_1 \leftarrow 3s^1S_0$ transition of matrix-isolated atomic magnesium for the first time. The strong 204.5 nm peak of Mg/Ar closely matches the position of the $4p^1P_1 \leftarrow 3s^1S_0$ transition of atomic magnesium in the gas phase. Other weaker peaks at 192.5 and 185 nm in Mg/Ar probably arise from spectrally resolved transitions of magnesium atoms with multiple site occupancy. On the basis of this assignment, site splittings on transitions to the $4p^1P_1$ level are much better resolved than in the lower-energy $3p^1P_1 \leftarrow 3s^1S_0$ transition. The reason for the well-resolved site splittings is probably due to the stronger Mg–RG host interactions involved in the $4p^1P_1$ state than in the $3p^1P_1$ state. On the other hand, the reason for the particularly strong $4p^1P_1 \leftarrow 3s^1S_0$ transition in argon compared with the other rare gas matrices is not immediately evident.

Emission from the $4p^1P_1$ level is not observed in any of the Mg/RG systems following excitation of the $4p^1P_1$ level but indirect emission from the $3p^1P_1$ level is observed. The

most likely mechanism for the population cascade from the $4p^1P_1$ level to $3p^1P_1$ level is curve crossing of a strongly bound state correlating to the $4p^1P_1$ asymptote by a repulsive Σ -type curve dissociating to the $3p^1P_1$ state.

In the Mg/Ar system, the small red shift on the $4p^1P_1 \leftarrow 3s^1S_0$ absorption is in contrast to the small blue shift on the $3p^1P_1 \leftarrow 3s^1S_0$ transition. This is probably arising from the strongly attractive $\text{Mg}(4p^1P_1) \cdot \text{Ar}^1\Pi$ molecular state. Spectroscopic studies on this state have not been carried out yet, but existing work on the doubly excited $\text{Mg}(3p^2^3P_J) \cdot \text{Ar}^3\Sigma$ state have revealed very strong bound interactions.

We would like to acknowledge Dr. Peter Gürtler and Mr. Sven Petersen for their technical assistance during the course of this work. This research was funded in part by the European Union, TMR 1996-'98, "Access to Large Scale Facilities" Program and by the Irish Government Forbairt Basic Science research scheme, to whom B. H. and P. K. also gratefully acknowledge receipt of Ph.D studentships.

*E-mail: jmccaffrey@may.ie

¹J. G. McCaffrey and P. N. Kerins, *J. Chem. Phys.* **106**, 7885 (1997).

²J. G. Kaup and W. H. Breckenridge, *J. Phys. Chem.* **99**, 13701 (1995).

³V. A. Bracken, P. Gürtler, and J. G. McCaffrey, *J. Chem. Phys.* **107**, 5290 (1997).

⁴J. Zuniga, A. Bastida, A. Requena, N. Halberstadt, and J. Beswick, *J. Chem. Phys.* **98**, 1007 (1993).

⁵W. H. Breckenridge, C. Jouviet, and B. Soep, "Metal-atom/rare-gas van der Waals complexes," in *Advances in Metal and Semiconductor Clusters*, Vol. III, edited by M. A. Duncan (JAI Press, Greenwich, 1995).

⁶S. Massick and W. H. Breckenridge, *J. Chem. Phys.* **105**, 6154 (1996).

⁷R. R. Bennett, J. G. McCaffrey, I. Wallace, D. J. Funk, A. Kowalski, and W. H. Breckenridge, *J. Chem. Phys.* **90**, 2139 (1989).

⁸J. R. Fuhr and W. L. Wiese, *Atomic Transition Probabilities*, 10, *CRC Handbook of Chemistry and Physics*, edited by David R. Lide, 76th ed., 1995–1996.

⁹C. E. Moore, *Atomic Energy Levels*, Vol. 1 (National Bureau of Standards Circular number 467, U.S. Government, printing office, Washington D.C., 1957).

¹⁰C. Crepin-Gilbert and A. Tramer, *Int. Rev. Phys. Chem.* **18**, 485 (1999).

¹¹O. Schnepp, *J. Phys. Chem. Solids* **17**, 188 (1961).

¹²L. Mowery, J. C. Miller, E. R. Krausz, P. N. Schatz, M. Jacobs, and L. Andrews, *J. Chem. Phys.* **70**, 3920 (1979).

¹³J. G. McCaffrey and G. A. Ozin, *J. Chem. Phys.* **101**, 10354 (1994).

¹⁴D. V. O'Connor and D. Phillips, *Time Correlated Single Photon Counting* (Academic Press, London, 1984).

¹⁵G. Zimmerer, *Nucl. Instrum. Methods Phys. Res. A* **308**, 178 (1991).

¹⁶"ZFIT" program *Nonlinear Least Squares Analysis of Fluorescence Decay Data* by M. Rehorek, H. Otto, W. Rettig, A. Klock, and modified by P. Gurtler and M. Joppien (last update, August 1995).

¹⁷J. G. McCaffrey, Ph.D. Thesis, Univ. of Toronto (1987).

¹⁸P. N. Kerins, M. Sc. Thesis, Nat. Univ. of Ireland, Maynooth, (1997).

¹⁹L. Andrews, W. W. Duley, and L. Brewer, *J. Mol. Spectrosc.* **70**, 41 (1978).

²⁰V. E. Bondybey, *J. Chem. Phys.* **68**, 1308 (1977).

²¹This expectation is based on the larger quantum defect exhibited by the orbitals with smaller orbital quantum numbers, *l*.

This article was published in English in the original Russian journal. Reproduced here with stylistic changes by the Translation Consultant.